NJC

Accepted Manuscript

This is an *Accepted Manuscript*, which has been through the Royal Society of Chemistry peer review process and has been accepted for publication.

Accepted Manuscripts are published online shortly after acceptance, before technical editing, formatting and proof reading. Using this free service, authors can make their results available to the community, in citable form, before we publish the edited article. We will replace this *Accepted Manuscript* with the edited and formatted *Advance Article* as soon as it is available.

You can find more information about *Accepted Manuscripts* in the Information for Authors.

Please note that technical editing may introduce minor changes to the text and/or graphics, which may alter content. The journal's standard Terms & Conditions and the Ethical guidelines still apply. In no event shall the Royal Society of Chemistry be held responsible for any errors or omissions in this *Accepted Manuscript* or any consequences arising from the use of any information it contains.

ROYAL SOCIETY OF CHEMISTRY

www.rsc.org/njc

NJC

RSCPublishing

PAPER

Effects of carbon nanomaterials on the aggregation of a bi-oxadiazole derivative (BOXD-T8) in DMF and its gel properties

Cite this: DOI:

Received
Accepted

DOI:

www.rsc.org/

Yan Zhang, Haitao Wang*,Yangfang Wu and Min Li*

Two different carbon nanomaterials (CNMs): single-walled carbon nanotubes (SWNTs) and graphene oxide (GO) were successfully incorporated into a bi-1,3,4-oxadiazole derivative (BOXD-T8) in DMF and gel. Molecules of BOXD-T8 self-assembled to *H*- and *J*-aggregates in DMF within moderate concentration, and the ratio of *H*- aggregates and *J*-aggregates could be manipulated simply by changing concentration. Energy transferred from *H*- aggregates to outputting CNMs might have been involved due to the incorporation of CNMs. Furthermore, the incorporation of SWNTs is better to induce aggregation of BOXD-T8, while GO is better to induce the formation of *J*-aggregation, which resulted in a lower critical gelation concentration (CGC) and different morphologies compared to those of the corresponding pure BOXD-T8 organogel. The SEM morphologies showed that SWNTs-containing hybrid xerogel consisted of spherical aggregates derived from the entanglement of fibers. In contrast, both graphene sheets and entangled fibers were observed for GO-containing hybrid xerogels. In addition, the composites gel showed improved mechanical properties due to the physical enhancement effects of the incorporated CNMs as rigid materials in the organogel network.

Introduction

In the last few years, one-dimensional carbon nanotubes (CNTs), especially single wall carbon nanotubes (SWCNTs), [1, 2] and two-dimensional graphene[3] are two kinds of the most studied carbon nanomaterials (CNMs). Much attention has been paid in the areas of solid state electronics[4, 5] and composite materials, [6, 7] due to their unique electronic,[8] optical,[9] thermal, [10]especially mechanical properties.[11,12] The CNMs can greatly affect the properties of the hosts through doping to other molecular building blocks. [13] Moreover, it is also a powerful strategy for improving the solubility of CNMs and in turn for introducing new properties.[14, 15, 16]

For example, Anderson and co-workers demonstrated that the incorporation of SWNTs into porphyrins solutions resulted in an electron donor–acceptor nanohybrids bearing light harvesters.[17] Low-molecular weight aromatic molecules, such as azobenzene chromophores, [18,19,20] and pyrene chromophores were also demonstrated to efficiently interact with SWNTs. According to Ito and co-workers' results, combining SWNTs to a pyrene derivative through π-π interaction generated a system with better photochemical, photovoltaic, and photocatalytic properties.[21] Graphene oxide (GO) were found to enhance the fluorescence of conjugated polyelectrolytes (CPEs) with charge transfer characteristics under certain conditions according to Liu and co-workers' work.[22]

Winey and co-workers reported the first organogel/carbon nanotubes (CNTs) composites which showed significant improvements in mechanical and electrical properties using 12-hydroxystearic acid (HSA) as the gelator.[23] Ye and co-workers demonstrated that addition of GO showed positive effects on the improvements of thermal and mechanical properties of poly (acrylic acid) (PAA) hydrogels.[24] Arindam Banerjee and co-workers reported a stable hybrid organogel system in which non-covalent π-π stacking interaction between pyrene-conjugated and graphene sheets was demonstrated.[25] They had also developed a convenient "green chemical" method to make a GO-based nanohybrid system within the hydrogel matrix.[26] In another paper, a graphene oxide/ hemoglobin composite hydrogel with high yields, exceptional

*Key Laboratory for Automobile Materials (JLU), Ministry of Education, College of Materials Science and Engineering, Jilin University, 2699 Qianjin Road, Changchun, 130012, P. R. China
E-mail: minli@mail.jlu.edu.cn, haitao_wang@jlu.edu.cn;
Tel: +86 431 85168254

activity and stability was prepared, and it had been used for catalyzing a peroxidatic reaction in organic solvents.[27]

1,3,4-oxadiazole derivatives, with 1,3,4-oxadiazole rings conjugated to phenyl rings, have been widely used in bioorganic and medicinal chemistry[28] and as electron-transporting/hole blocking (ETHB) materials[29,30] for OLEDs, due to their electron-deficient nature, high photoluminescence quantum yield(PLQY), and high thermal stabilities.[31]

In our previous work, we reported a bi-1,3,4-oxadiazole derivative (BOXD-T8) (Scheme 1), which showed intermolecular charge transition at certain concentration range.[32, 33] Our present work demonstrated that the energy transfer may be involved in BOXD-T8/SWNTs and BOXD-T8/GO composites in solution. It was demonstrated that BOXD-T8/CNM organogels showed reinforced aggregation.

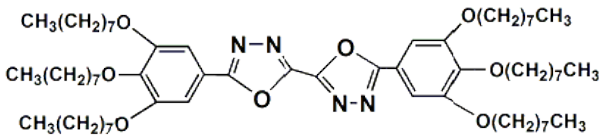

Scheme 1 Molecular structure of BOXD-T8 organogelator

Experimental

Materials

The gelator BOXD-T8 was synthesized according to the literature methods.[32] Its structure was characterized by FT-IR, ^{1}H NMR spectroscopy and elemental analysis (see electronic supplementary information). SWNTs were purchased from Shenzhen Nanotech Port Co., Ltd, having an outer diameter of 10-20 nm and length <2 μm. The purity is more than 97%. Graphene oxide (GO) and all reagents obtained from commercial sources and used without further purification.

Characterization

^{1}H NMR spectra were recorded with Bruker Avance 500 MHz spectrometer, using $CDCl_3$ as a solvent and tetramethylsilane (TMS) as an internal standard. FT-IR measurements were recorded on a Perkin–Elmer spectrometer (Spectrum One B). The xerogel samples for FT-IR were prepared with KBr to form transparent pellets. X-ray diffraction (XRD) measurements were carried out with a Bruker Avance D8 X-ray diffractometer(Cu, Kα radiation, λ=1.54 Å). SEM observations were taken with a SSX-550 apparatus. Samples for this measurement were prepared by wiping a small amount of the organogel or a drop of solution on silica plate and dried at room temperature. All the samples were coated by gold before observation. The rheological measurements were performed using a TA instrument (AR2000 Rheometer) with 40 mm parallel plate geometry. The samples were sandwiched between the two plates with a gap of 0.5 mm throughout the experiments. The linear viscoelastic regime (LVR) of deformations of the gels was determined with a strain amplitude test ranging from 0.01% to 100%. Afterward, the gels were subjected to the frequency sweep test, the storage modulus (G') and the loss modulus (G'') are monitored as a function of applied frequency under a constant strain 0.1%. Photoluminescence spectra were collected by a Perkin-Elmer LS55 fluorescence spectrophotometer and UV/vis absorption spectra were performed using a Shimadzu UV-2550 spectrometer with 1.0x1.0 cm quartz cells.

Preparation of organogel in DMF

Organogel was prepared by mixing certain amount of BOXD-T8 in DMF in a sample vial. The mixture was heated to solution and then cooled down at room temperature. Gelation was considered to occur when the test tube can be turned upside down without fluid. Critical gelation concentration (CGC) was determined by weighing up a minimum amount of gelator needed for the formation of a stable gel.

Typical preparation procedure for the hybrid organogel as follows: with the aid of ultrasound treatment (2 h), either SWNTs or GO was dispersed in DMF separately. Then a fixed amount of BOXD-T8 was added to the well dispersed solution and heated. The mixture was re-sonicated for 5 min at ca. 50 ℃ and then quenched to room temperature.

Determine of T_{gel}

Gel-to-sol transition temperatures (T_{gel}) were determined by using a conventional ''falling ball'' method. In the test, organogels were prepared in test tubes and carefully put upside down in a thermostatted water bath with the temperature raised slowly. The temperature at which the last tiny part of gel was completely dissolved was taken as the T_{gel} of the system.

Results and discussion

Our previous study has demonstrated that the BOXD-T8 can be well dissolved in ethanol and DMF.[32] Here we choose DMF as solvent because SWNTs and GO can be well dispersed in DMF with the aid of ultrasound treatment.

Fluorescence study

As shown in Figure 1a, BOXD-T8 showed a strong emission peak at 485 nm in DMF ($1x10^{-6}$ mol/L), and its maximum emission is independent of concentration within $1x10^{-6}$ to $1x10^{-4}$ mol/L. In contrast, the fluorescence intensity of BOXD-T8 dropped dramatically upon addition of GO (0.06 mg/mL) and SWNTs (0.06 mg/mL) in DMF (Figure 1b). The fluorescence intensity decreased by 37 times for BOXD-T8/SWNTs compared to that of BOXD-T8, while that of BOXD-T8/GO was 1.8 times.

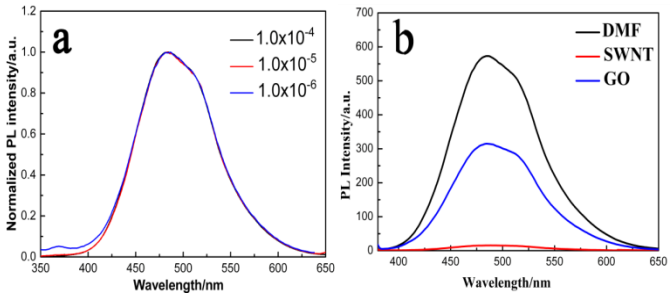

Figure 1a: Normalized concentration-dependent emission spectra of BOXD-T8 in DMF (mol/L); b: Fluorescence emission spectra of BOXD-T8 and its composites with 0.06 mg /mL SWNTs and 0.06 mg/mL GO in DMF (1x10^{-4} mol/L).

Fluorescence excitation measurement, which is more sensitive to the electron distribution of the molecule in the ground state [34, 35], was further conducted for BOXD-T8 and the composites in DMF.

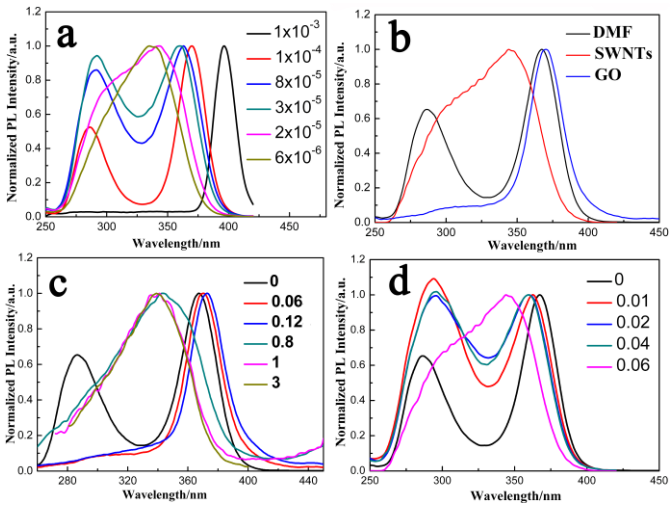

Figure 2a: Normalized concentration-dependent fluorescence excitation spectra of BOXD-T8 in DMF (mol/L) recorded at λ_{em} =485 nm. Normalized fluorescence excitation spectra of BOXD-T8 in DMF (1x10^{-4} mol/L) recorded at λ_{em}=485 nm b: in the absence and in the presence of 0.06 mg /mL SWNTs and 0.06 mg/mL GO, respectively; c: with variable GO concentration (mg/mL); d: with variable SWNTs concentration (mg/mL).

As shown in Figure 2a, BOXD-T8 exhibited a single peak at 335 nm, strongly indicated that BOXD-T8 are molecularly dissolved in DMF at low concentration (lower than 6x10^{-6} mol/L). At 3x10^{-5} mol/L, two new bands were observed, one blue-shifted by about 42 nm with respect to the monomer band, and the other one red-shifted by about 25 nm, indicating the simultaneous formation of *H*- and *J*-aggregates. The intensity of excitation at 292 nm (*H*-aggregates) decreased, and finally disappeared, while the excitation at 360 nm (*J*-aggregates) red-shifted gradually to 397 nm with the concentration increased to 1x10^{-3} mol/L. The *H*-aggregates are generally non-emissive, however, in this case the excitations at 292 nm (*H*-aggregates) and 360 nm (*J*-aggregates) could both give the emission at 485 nm, which strongly suggests that energy transfer from *H*- to *J*-aggregates might have been involved. The composites BOXD-T8/SWNTs (0.06 mg/mL) at 1x10^{-4} mol/L showed a broad excitation at 344 nm instead of two, suggesting BOXD-T8 molecules in solution were molecularly dispersed. So it is reasonable to predict that some BOXD-T8 molecules participate due to the incorporation of SWNTs, resulted in a decrease of the dissolved amount. While for the case of GO-incorporated system, the peak at 292 nm was missing, indicating the disappearance of *H*-aggregates. At the same time, the excitation peak at 360 nm hardly changed.

Figure 2c displayed the fluorescence excitation spectra of BOXD-T8 (10^{-4} mol/L) in presence of different amount of GO. It can be seen that at low concentration of GO (less than 0.12 mg/mL), one excitation peak at ca. 372 nm (*J*-aggregates) was observed, while for higher concentrations of GO (such as 0.8, 1and 3 mg/mL), only one broad peak was observed at 340 nm instead of two peaks. These results strongly suggested that the incorporation of a small amount of GO will favor the formation of *J*-aggregation. With the increase of GO concentration, BOXD-T8 will tend to form aggregates. So the dissolved amount became less and less, resulting in a molecularly dissolved solution. Similarly, BOXD-T8/SWNTs composite showed one broad peak at 340nm at higher SWNTs (0.06mg/mL) in DMF, indicating that BOXD-T8 is molecularly dissolved.

After comparing the cases between SWNT- and GO-incorporated solutions, it could be easily noticed that SWNTs is better to induce aggregation, while GO is better to induce the formation of *J*-aggregation.

UV/vis absorption spectra

As shown in Figure 3a, BOXD-T8 in DMF (2.5x10^{-5} mol/L) showed a strong absorption maximum at 327 nm, whose intensity increased with concentrations up to 2.0x10^{-4} mol/L. The composite BOXD-T8/SWNTs in DMF showed gradually red-shifted absorption from 327 nm to 336 nm with the increase of SWNTs concentration. Similar spectral change was observed in BOXD-T8/GO system, and the red-shift was 14 nm. The red shift indicated changes in energy level upon addition of the SWNTs and GO into the BOXD-T8 solutions in DMF. The elevated baselines were due to the presence of CNMs.

We measured the UV-vis spectra of the SWNTs/BOXD-T8 and GO/BOXD-T8 in DMF with a fixed SWNTs or GO concentration, but different BOXD-T8 concentration (Figure S6). It showed that (Figure S1c) the maximum absorption red-shifted from 320 nm to 346 nm, with the increase of concentration from 8.0x10^{-6} mol/L to 1.2x10^{-4} mol/L in the presence of 0.4 mg/mL GO, suggesting that GO induced *J*-aggregation among BOXD-T8 molecules. In the case of BOXD-T8/SWNTs composites, the absorption peak red-shifted about 15 nm with the increase of BOXD-T8 concentrations at 0.04 mg/mL of SWNTs (Figure S1b).

So it was reasonable to predict that energy transfer from *H*-aggregates to outputting CNMs might have been involved.

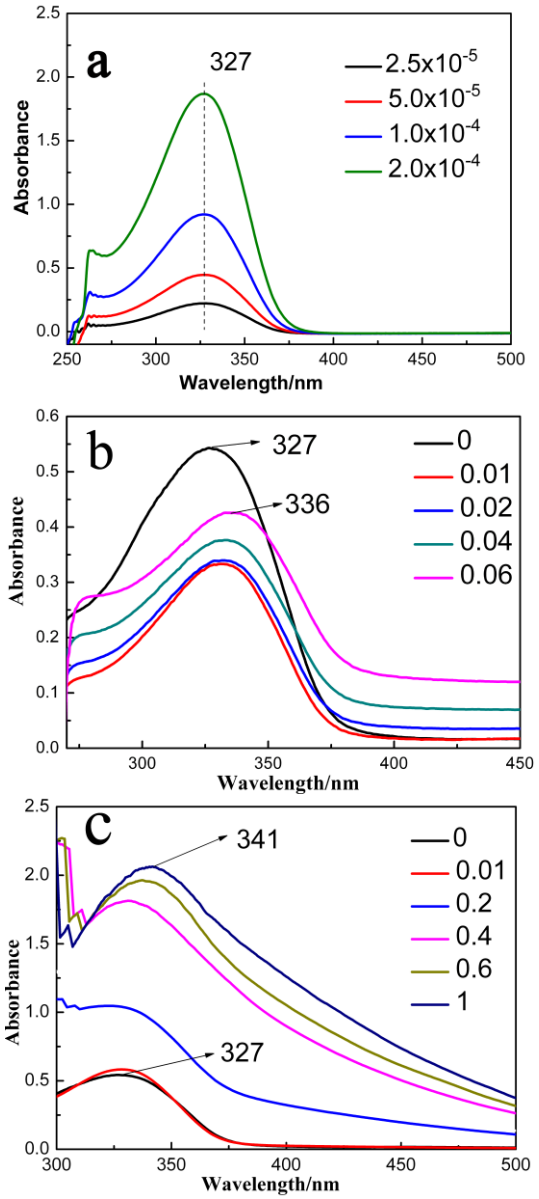

Figure 3 Concentration variation (mol/L) UV/vis absorption spectra of BOXD-T8 in DMF (a), UV/vis spectra of BOXD-T8 in DMF at a fixed concentration of $1x10^{-5}$ mol/L with different amount of SWNTs (b) and GO (c). The unit for the values is mg/mL.

Gel formation

The un-doped gel and hybrid gel (as shown in Figure 4a-c) were all thermo-reversible and were stable at room temperature for several weeks. SWNTs could only be incorporated as much as 0.06 mg/mL beyond which it would tend to precipitate. While the maximum GO dispersed in the gel network was 3 mg/mL without losing its gelation ability.

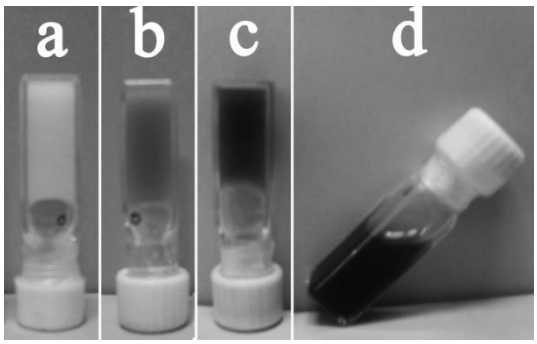

Figure 4 Photographs of DMF gel of a: BOXD-T8 (6 mg/mL); b: BOXD-T8 (6 mg/mL) and SWNTs (0.06 mg/mL) mixture; c: BOXD-T8 (6 mg/mL) and GO (3 mg/mL) mixture. d: GO dispersion in DMF (3 mg/mL).

Effects of SWNTs and GO on CGC and T_{gel}

As shown in Figure 5, the critical gelation concentration (CGC) of BOXD-T8 in DMF is 0.61wt%, while it decreased to 0.15 and 0.11wt% when 0.06 mg/mL SWNTs and 0.1 mg/mL GO were added respectively. While CGC changed a little with the increase of GO amount (Figure 5), and the CGC of the hybrid gel decreased to 0.07wt%, at 1 mg/mL GO addition, e.g. only about ten percent of the amount needed for the original un-doped gel. This is all reasonable based on the fluorescence results: with the incorporation of CNMs, more BOXD-T8 molecules tended to form aggregates, so the amount of BOXD-T8 dissolved in solution was reduced, resulting in the decreases of CGC.

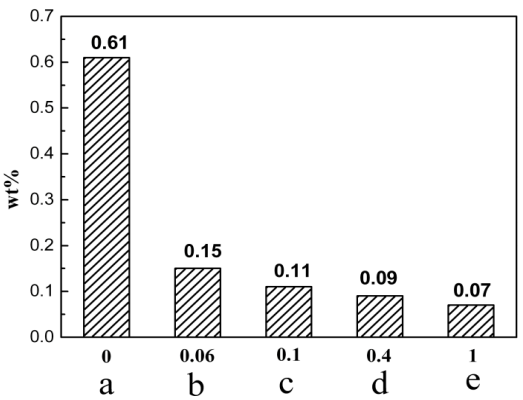

Figure 5 Histogram of the CGC of DMF gel of BOXD-T8 in different concentration of CNMs. a: the case of un-doped gel; b: the case of 0.06mg/mL SWNTs incorporated gel, c-f: the case of GO incorporated gel. Unit of the value on the horizontal ordinate is mg/mL.

Figure 6a showed the plots of gel-sol transition temperature (T_{gel}) of both un-doped and CNM-doped gels at different concentrations. It can be found that all these gels showed a similar trend: T_{gel} raised as the gelator concentration increased until a plateau value was reached, denoted by a concentration-independent gel. Incorporation of both SWNTs and GO stabilized the gels. For example, T_{gel} value for the un-doped gel is 42 ℃ at 0.019 mol/L of BOXD-T8，while 49, 56 ℃for SWNTs-and GO-doped gels, respectively. In addition, organogels incorporating SWNTs possessed the largest gel-sol

transition enthalpy (Figure S2) and the highest T_{gel} values all through the concentration tested. Figure 6b showed that the amounts of GO did have some influence on the T_{gel} values, especially in relatively high concentration region (> 0.007 mol/L, for this system): the more GO amount, the higher T_{gel} values at the same BOXD-T8 concentration. These results suggested that the fibrillar network of the BOXD-T8/CNMs gels might be much stronger, and it would require higher temperature to disintegrate the self-assemble networks compared to that of the un-doped gel.

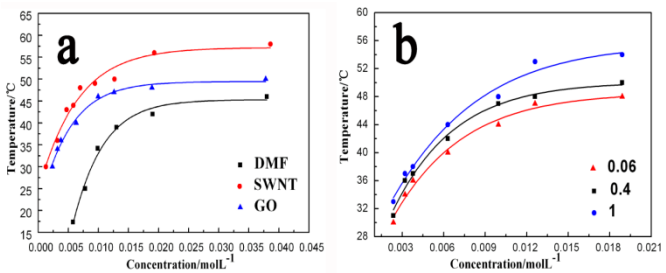

Figure 6 Dependence of the gel-sol phase transition temperature, T_{gel}, upon the gelator concentrations, a: with different incorporations, the concentration of SWNT and GO is 0.06 mg/mL; b: with variable GO concentrations (mg/mL).

Morphology

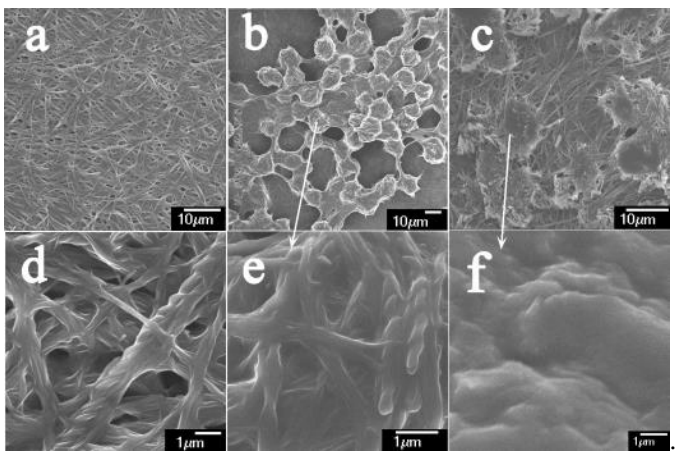

Figure 7 SEM images of DMF xerogels of (a) BOXD-T8 (6 mg/mL); (b) BOXD-T8 and SWNTs (0.06 mg/mL) mixture; (c) BOXD-T8 and GO (1 mg/mL) mixture. Images of (d), (e) and (f) showed the enlarged version of (a), (b) and (c) respectively.

To get a better insight into the supra-molecular arrangements of the composites organogel, Scanning Electron Microscopic (SEM) study on the xerogels was carried out. Firstly, it was worth to note that SWNTs in DMF were found to be well dispersed, with outer diameter of 10-20 nm (Figure S3a). And GO sheets were found to show different layers. Some showed flexible structures with fewer layers, the others are thicker structures due to aggregation of GO sheets (Figure S3b, c).

As shown in Figure 7a, the xerogel of the un-doped BOXD-T8 gel in DMF showed a three-dimensional fibrous network. The width of the fibers was within the range of 0.2-0.5 μm, and the fibers were highly entangled with each other (as shown in Figure 7d). Interestingly, when a small amount (0.06 mg/mL) of SWNTs was added, spherical aggregates with a diameter about 10 μm were observed (as shown in Figure 7b). An enlarged version of the structures (Figure 7e) showed that spherical aggregates consist of entangled fibers, whose dimensions were similar to that of the BOXD-T8 gel. Considering the small size of SWNTs and a heterogeneous nucleation process, we predict that the SWNTs were packed inside the spherical aggregates. Upon incorporating 1 mg/mL GO into the organogel, the resulting composites exhibited both GO sheets and entangled fibers (Figure 7c). The diameter of the fibers remained almost the same, suggesting that the incorporating didn't affect the regular self-assembly of BOXD-T8. Interestingly, the fibers of the GO incorporated gel showed a clear alignment with densely packed networks on the surface of GO sheets (Figure 7f) compared to the flat surface of pure GO sheets. To ensure whether there are some interactions between fibers and GO sheets, morphology of mixture of BOXD-T8 and GO was also examined in its solution state (10^{-4} mol/L). As shown in Figure S4, there were some fibers crossed over the surface of GO sheets, which revealed that molecules of BOXD-T8 interacted well with the GO sheets and the GO-incorporated organogel was a true composite system. From a different perspective, the shapes and diameters of the two-dimension sheet of GO were not capable of prevent the molecules from self-assembled into fiber aggregates.

FT-IR and XRD studies

To further investigate whether CNMs affected the interactions among molecules of BOXD-T8, FT-IR spectra of both un-doped and hybrid xerogels were measured. As shown in Figure 8, the BOXD-T8 xerogel showed strong anti-symmetric and symmetric CH_2 stretching vibrations at 2923 and 2853 cm^{-1}, suggesting the presence of gauche conformation in the alkyl chains. It can be seen that the xerogels of the composites showed almost the same absorption bands, which suggest that the molecular interactions among gelator molecules remain un-changed. A characteristic absorption band of GO at 1728 cm^{-1} was observed for the BOXD-T8/GO composites xerogel.

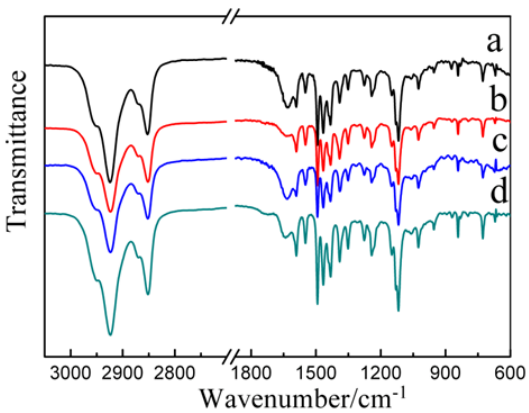

Figure 8 FT-IR spectra of xerogels of (a) BOXD-T8 (6 mg/mL); (b) BOXD-T8 (6 mg/mL) and SWNTs (0.06 mg/mL) mixture; (c) BOXD-T8 (6 mg/mL) and GO (0.06 mg/mL) mixture; (d) BOXD-T8 (6 mg/mL) and GO (1 mg/mL) mixture.

The XRD profile of BOXD-T8 xerogel from DMF (Figure 9) consisted of three peaks (d=19.53, 14.28, 13.03 Å) in the small-angle region and several peaks in the wide-angle region, suggesting its crystalline feature. The xerogels from the composites exhibited the similar XRD profiles, indicating the same packing mode of BOXD-T8 in the composites. As indicated by SEM images, xerogels of the incorporated samples consisted of similar fiber structures with the same width compared to the un-doped ones, so the incorporation didn't have remarkable impacts on the regular self-assembly of BOXD-T8, resulting in a similar packing pattern. From the other aspect, the diameters of SWNTs (or GO) are not so matched with BOXD-T8 molecules. It would be a little difficult to affect the self-assembly in molecular scale. It is worth to note that, the XRD pattern of xerogels of BOXD-T8 with 1 mg/mL GO presented a sharp diffraction peak at 2theta=10.3 °, which is a characteristic diffraction peak of GO.

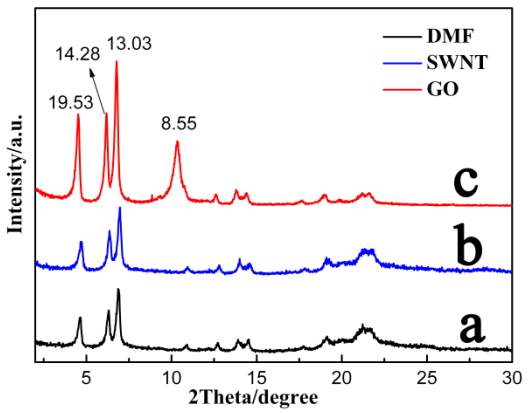

Figure 9 XRD spectra of xerogels of (a) BOXD-T8 (6 mg/mL); (b) BOXD-T8 (6 mg/mL) and SWNTs (0.06 mg/mL) mixture; (c) BOXD-T8 (6 mg/mL) and GO (0.06 mg/mL) mixture.

Based on the SEM, FT-IR and XRD results, it is reasonable to illustrate that either intermolecular interaction or the molecular packing of BOXD-T8 remained unchanged upon incorporation of CNMs to its gels.

Rheological property

To examine the influence of CNMs on the fluidity and rigidity of the composites organogels, mechanical properties of organogels were characterized by mechanical rheometry at 25 ℃, shown in Figure 10. The storage modulus (G') described the ability of the deformed materials to store energy, and the loss modulus (*G''*) corresponded to the ability of the material to dissipate energy.[36] Under oscillatory frequency sweep experiments, *G'* was always higher than G'' over the entire frequency range (0.1-100 Hz) at 0.1% strain amplitude for all gels, indicating their elastic structures. While for BOXD-T8 gel, both *G'* and *G''* showed largely dependency on the frequency, indicating its poor strength. Interestingly, upon incorporating 0.06 mg/mL SWNTs into the organogel, the linear viscoelastic regime (LVR) was broadened and the value of yield strain was enlarged. Both *G'* and *G''* of the BOXD-T8/SWNTs composite gel showed frequency-independence through the frequency range, while the *G'* value reached to 3078 Pa, which is 9.3 times of that of BOXD-T8 gel (333 Pa) at the same concentration (1 Hz, 0.1%). The increases in G', G'' and yield strain were also observed in BOXD-T8/GO gel: G' value reached to 1187 Pa (3.6 times). The composites gel showed improved mechanical properties. And when incorporated the same amount of SWNTs and GO, small amount of SWNTs could give relatively larger reinforcement of stiffness and elastic properties. And the mechanical difference could also be explained in view of the original differences between the two CNMs: the tube-like structure of SWNTs is more similar to fibre structure not only on diameter but also on dimension (one-dimension), which made them more compatible in the self-assemble network, resulting in a more rigid and stable structure.

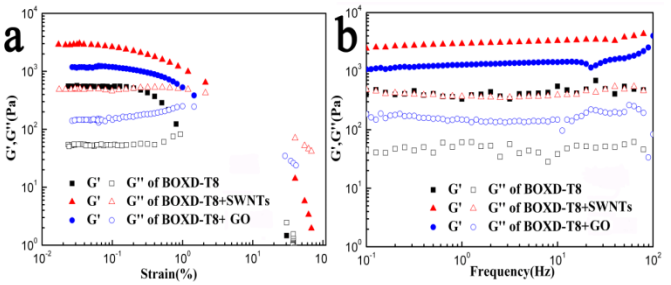

Figure 10 Amplitude (a) and frequency (b) dependencies of the storage modulus (G') and loss modulus (G'') of DMF gels of BOXD-T8 (6 mg/mL), BOXD-T8 and SWNTs (0.06 mg/mL) mixture and BOXD-T8 and GO (0.06 mg/mL) mixture, respectively. The frequency is 1 Hz and the strain is 0.1%.

Figure 11 showed the frequency-dependent G' of the gels with different amount of GO. It showed that a gradual increase in both G' and G'' was observed with the increase of GO: G' of the gel with 0.06 mg/mL GO reached to 1187 Pa (3.6 times, compared to that of the BOXD-T8 gel), and 3010 Pa (ca. 9.0 times) for that with 3 mg/mL GO. This indicated that the physical enhancement effects of the incorporated CNMs as rigid materials was another reason for the formation of a more rigid and elastic gel when subjected to external forces.

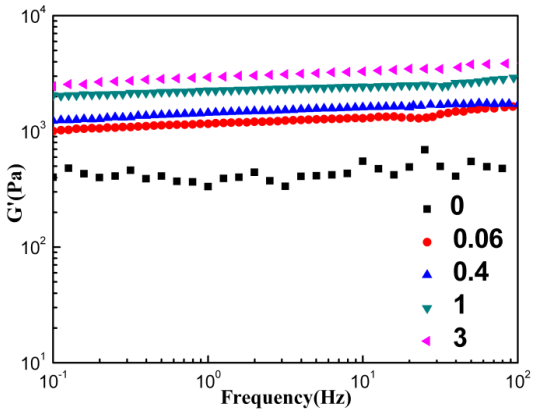

Figure 11 Plot of G' of DMF gels of BOXD-T8 (6 mg/mL) and GO mixture as a function of frequency with varying GO amounts (0-3 mg/mL).

Conclusions

Interestingly, we found the incorporation of carbon nanomaterials had significant effects on not only the fluorescence spectra of BOXD-T8 in DMF but also gel behaviors. An interesting aggregation mode was found for BOXD-T8 in DMF: transformation of *H*-aggregates into *J*-aggregates could manipulate simply by increasing concentration. When carbon nanomaterials were added into the solution, energy transfer from *H*- aggregates to outputting carbon nanomaterials might have been involved. Furthermore, the incorporation of SWNTs is better to induce aggregation, while GO is better to induce the formation of *J*-aggregation which resulted in a lower critical gelation concentration and different aggregation morphologies compared to those of the corresponding BOXD-T8 organogel. The rheological study revealed that both G' and G'' were higher for hybrid gels compared to the BOXD-T8 gels, indicating formation of a stronger solid like network due to the physical enhancement effects of the incorporated carbon nanomaterials as rigid materials. While SWNTs could affect the gel in a more mechanical way, owing to the one-dimensional tube-like structures.

Acknowledgements

The authors are grateful to the National Science Foundation Committee of China (Project Nos. 51073071, 21072076 and 51103057), and Project 985-Automotive Engineering of Jilin University for financial support of this work.

Notes and references

1 S. Iijima, *Nature*, 1991, **354**, 56.
2 S. Iijima and T. Ichihashi, *Nature*, 1993, **363**, 603.
3 K. S. Novoselov, A. K. Geim, S. V. Morozov, D. Jiang, Y. Zhang, S. V. Dubonos, I. V. Grigorieva and A. A. Firsov, *Science*, 2004, **306**, 666.
4 X. Li, X. Wang, L. Zhang, S. Lee and H. Dai, *Science*, 2008, **319**, 1229.
5 Y. Zhang, J. W. Tan, H. L. Stormer and P. Kim, *Nature*, 2005, **438**, 201.
6 S. Watcharotone, D. A. Dikin, S. Stankovich, R. Piner, I. Jung, G. H. B. Dommett, G. Evmenenko, S. E. Wu, S. F. Chen, C. P. Liu, S. T. Nguyen and R. S. Ruoff, *Nano Lett.* 2007, **7**, 1888.
7 S. Stankovich, D. A. Dikin, G. H. B. Dommett, K. M. Kohlhaas, E. J. Zimney, E. A. Stach, R. D. Piner, S. T. Nguyen and R. S. Ruoff, *Nature*, 2006, **442**, 282.
8 T. Ando, *NPG Asia Mater.*, 2009, **1**, 17.
9 H. X. Chang and H. K. Wu, *Adv. Funct. Mater.*, 2013, **23**, 1984.
10 S.W. Kim, H.K. Jeong, Y.G. Kang and M.H. Han, *Asian J. Chem.* 2013, **25**, 9, 5153.
11 S. Srinivasan, S. S. Babu, V. K. Praveen and A. Ajayaghosh, *Angew. Chem.*, 2008, **120**, 5830.
12 B. S. Shim, W. Chen, R. C. Doty, C. Xu and N. A. Kotov, *Nano Lett.*, 2008, **8**, 4151.
13 K. Dirian, M. Herranz, G. Katsukis, J. Malig, L. R. P´erez, C. R Nieto, V. Strauss, N. Mart´ın and D. M. Guldi, *Chem. Sci.*, 2013, **4**, 4335.
14 D. R. Kauffman and A. Star, *Chem. Soc. Rev.*, 2008, **37**, 1197.
15 D. A. Heller, H. Jin, B. M. Martinez, D. Patel, B. M. Miller, T. K. Yeung, P. V. Jena, C. Hbartner, T. Ha, S. K. Silverman and M. S. Strano, *Nat. Nanotechnol.*, 2009, **4**, 114.
16 H. Bai, C. Li, X.L.Wang, and G.Q. Shi, J. Phys. Chem. C, 2011, 115, 5545.
17 J. K. Sprafke, S. D. Stranks, J. H. Warner, R. J. Nicholas and H. L. Anderson, *Angew. Chem. Int. Ed.*, 2011, **50**, 2313.
18 C. Huang, R. K. Wang, B. M. Wong, D. J. McGee, F. Le´onard, Y. J. Kim, K. F. Johnson, M. S. Arnold, M. A. Eriksson and P. Gopalan, *Acsnano*, 2011, **5**, 7767.
19 A. Setaro, P. Bluemmel, C. Maity, S. Hecht and S. Reich, *Adv. Funct. Mater.*, 2012, **22**, 2425.
20 D. Canevet, A. Perez del Pino, D. B. Amabilino and M. Salle, *Nanoscale*, 2011, **3**, 2898.
21 F. D'Souza, A. S. D. Sandanayaka and O. Ito, *J. Phys. Chem. Lett.*, 2010, **1**, 2586.
22 J. L. Geng, L. Zhou and B. Liu, *Chem. Commun.*, 2013, **49**, 4818.
23 M. Moniruzzaman, A. Sahin and K. I. Winey, *Carbon*, 2009, **47**, 645.
24 J. F. Shen, B. Yan, T. Li, Y. Long, N. Li and M. X. Ye, *Soft Matter*, 2012, **8**, 1831.
25 B. Adhikari, J. Nanda and A. Banerjee, *Chem. Eur. J.*, 2011, **17**, 11488.
26 B. Adhikari, A. Biswas, and A. Banerjee, *Langmuir*, 2012, **28**, 1460.
27 C.C. Huang, H. Bai, C. Li and G.Q. Shi, *Chem. Commun*., 2011, **47**, 4962.
28 B. Narayanaa, K. K. V. Raja, B. V. Ashalathaa and N. S. Kumarib, *Arch. Pharm. Chem. Life Sci.*, 2005, **338**, 373.
29 C. Risko, E. Zojer, P. Brocorens, S. R. Marder and J. L.Bredas, *Chem. Phys.*, 2005, **313**, 151.
30 P. Zhao, X. Zhu, J. Chen, D. Ma and W. Huang, *Synth. Met.*, 2006, **156**, 763.
31 G. Hughes and M. R. Bryce, *J. Mater. Chem.*, 2005, **15**, 94.
32 S. N. Qu, L. J. Wang, X. Y. Liu and M. Li, *Chem. Eur. J.*, 2011, **17**, 3512.
33 S.N. Qu, L. J. Zhao, Z. X. Yu, Z. Y. Xiu, C. X. Zhao, P. Zhang, B. H. Long and M. Li, *Langmuir*, 2009, **25**, 1713.
34 B. Valeur, Molecular Fluorescence: Principles and Applications, Wiley-VCH Verlag GmbH 2001.
35 J. R. Albani, Structure and Dynamics of Macromolecules: Absorption and Fluorescence Sudies. Elsevier, Amsterdam, 2004.
36 H. A. Barnes, J. F. Hutton and F.R.S.Walters, An Introduction To Rheology, Third impression, P. O. Box 211,1000, AE Amsterdam, The Netherlands 1993.